

# The Preparation and Luminescence Decay Dynamics of Coupled Heterolanthanide(III) Cations in Dinuclear Schiff-base Complexes†

Karen D. Matthews,<sup>a</sup> Richard A. Fairman,<sup>a</sup> Andrea Johnson,<sup>b</sup> Kirk V. N. Spence,<sup>a</sup> Ishenkumba A. Kahwa,<sup>\*a</sup> Gary L. McPherson<sup>c</sup> and Hilary Robotham<sup>b</sup>

<sup>a</sup> Chemistry Department, University of the West Indies, Mona, Kingston 7, Jamaica

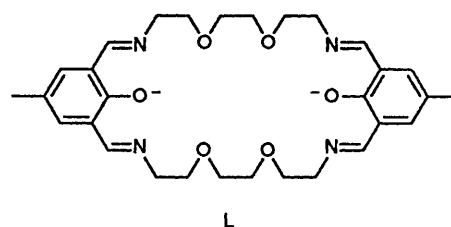
<sup>b</sup> Center for Nuclear Sciences, University of the West Indies, Mona, Kingston 7, Jamaica

<sup>c</sup> Chemistry Department, Tulane University, New Orleans, Louisiana 70118, USA

Molecular recognition events in which lanthanide(III) ( $\text{Ln}^{3+}$ ) cation pairs are formed have been studied using the template condensation crystalline products  $(\text{Ln}_{1-x}\text{Eu}_x)_2\text{L}(\text{NO}_3)_4 \cdot \text{H}_2\text{O}$  and  $(\text{Ln}_{1-x}\text{Tb}_x)_2\text{L}(\text{NO}_3)_4 \cdot \text{H}_2\text{O}$  (where  $\text{H}_2\text{L}$  is the [2 + 2] macrocyclic Schiff base obtained from 2,6-diformyl-*p*-cresol and 3,6-dioxaoctane-1,8-diamine). The observed relationship between the concentrations of  $\text{Eu}^{3+}$  (or  $\text{Tb}^{3+}$ ) in the reaction mixture  $X_{\text{Eu}}$  or  $X_{\text{Tb}}$  (from neutron activation analyses) with corresponding concentrations in the crystalline products ( $x$ ) suggests that formation of  $\text{LnEuL}(\text{NO}_3)_4 \cdot \text{H}_2\text{O}$  heteromolecules is more favourable than that of  $\text{LnTbL}(\text{NO}_3)_4 \cdot \text{H}_2\text{O}$ . In both cases the cation discrimination index, computed as the ratio of probabilities of  $\text{Ln}^{3+}$  incorporation into the crystalline heterolanthanide compounds, is in favour of the larger  $\text{Ln}^{3+}$  ion. However indiscriminate complexation of  $\text{Nd}^{3+}$  and  $\text{Eu}^{3+}$  in the  $(\text{Nd}_{1-x}\text{Eu}_x)_2\text{L}(\text{NO}_3)_4 \cdot \text{H}_2\text{O}$  system is unusual and reflects the importance of co-operative heteropair effects. Luminescence decay dynamics of the  $(\text{Sm}_{1-x}\text{Eu}_x)_2\text{L}(\text{NO}_3)_4 \cdot \text{H}_2\text{O}$  and  $(\text{Pr}_{1-x}\text{Tb}_x)_2\text{L}(\text{NO}_3)_4 \cdot \text{H}_2\text{O}$  systems ( $0 < x < 1$ ) reveal two microscopic environments for  $\text{Eu}^{3+}$  and  $\text{Tb}^{3+}$  which were attributed to homodinuclear molecules,  $\text{Ln}_2\text{L}(\text{NO}_3)_4 \cdot \text{H}_2\text{O}$  ( $\text{Ln} = \text{Eu}$  or  $\text{Tb}$ ) (slow component) and heterodinuclear molecules  $\text{SmEuL}(\text{NO}_3)_4 \cdot \text{H}_2\text{O}$  and  $\text{PrTbL}(\text{NO}_3)_4 \cdot \text{H}_2\text{O}$  (fast component). The luminescence decay rate constants for intramolecularly coupled  $\text{Eu-Sm}$  and  $\text{Pr-Tb}$  pairs are 8200 and 12 500  $\text{s}^{-1}$ , which yield coupling constants ( $\alpha$ ) of  $2.9 \times 10^{-53}$  and  $4.7 \times 10^{-53} \text{ m}^6 \text{ s}^{-1}$  respectively when dominant dipolar interactions are assumed. No exchange interactions are evident despite the presence of a phenolate linkage shared by the heteroatoms only  $\approx 4 \text{ \AA}$  apart. The ratio of  $\text{Eu-Eu}$  to  $\text{Eu-Sm}$  'cation pairing selectivity' constants of 1:1.5 (expected ratio for random pairing is 1:2) supports the intervention of molecular recognition processes favouring the homo- to hetero-paired species in the ion pairing events leading to  $(\text{Sm}_{1-x}\text{Eu}_x)_2\text{L}(\text{NO}_3)_4 \cdot \text{H}_2\text{O}$  compounds.

Dinuclear lanthanide(III) ( $\text{Ln}^{3+}$ ) complexes are important as potential new biomedical metallo-diagnostic<sup>1-6</sup> and therapeutic agents.<sup>7,8</sup> Possible applications of immobilized dinucleating chelates for the efficient separation and purification of lanthanides<sup>9</sup> are also of great interest. Whereas some dinuclear lanthanide complexes have been prepared,<sup>10-15</sup> especially by template procedures, essential information about molecular recognition processes which govern the  $\text{Ln}^{3+}$  cation pairing events is not available. Of particular interest are processes in which heterolanthanide cation pairs ( $\text{Ln-Ln}'$ ) are formed. Pure molecules which incorporate  $\text{Ln-Ln}'$  species are desirable as precursors to ternary metal oxides<sup>16</sup> with potentially important catalytic<sup>17</sup> and phosphor<sup>18</sup> characteristics which take advantage of mutual electronic interactions. Furthermore, biomedical benefits associated with coupling the functions of a potential therapeutic radionuclide<sup>8</sup> such as  $^{90}\text{Y}$  with those of a luminescent probe<sup>9</sup> ( $\text{Tb}^{3+}$  or  $\text{Eu}^{3+}$ )<sup>19,20</sup> in the same heterolanthanide dinuclear molecule can be envisaged. For these reasons better understanding of the chemistry and spectroscopy of coupled  $\text{Ln-Ln}'$  species is required. We have studied competitive binding events leading to the formation of heterolanthanide dinuclear complexes  $(\text{Ln}_{1-x}\text{Ln}'_x)_2\text{L}(\text{NO}_3)_4 \cdot \text{H}_2\text{O}$  and luminescence decay dynamics of the crystalline products.

Here we report the formation of heterodinuclear lanthanide-



(III) complexes  $(\text{Ln}_{1-x}\text{Eu}_x)_2\text{L}(\text{NO}_3)_4 \cdot \text{H}_2\text{O}$  and  $(\text{Ln}_{1-x}\text{Tb}_x)_2\text{L}(\text{NO}_3)_4 \cdot \text{H}_2\text{O}$  and their luminescence decay dynamics which reveal the presence of  $\text{Ln}^{3+}\text{-Eu}^{3+}$  and  $\text{Ln}^{3+}\text{-Tb}^{3+}$  heteropairs.

## Experimental

**Preparation of the Heterodinuclear Complexes.**—The complexes  $(\text{Ln}_{1-x}\text{Eu}_x)_2\text{L}(\text{NO}_3)_4 \cdot \text{H}_2\text{O}$  and  $(\text{Ln}_{1-x}\text{Tb}_x)_2\text{L}(\text{NO}_3)_4 \cdot \text{H}_2\text{O}$  were prepared by the template condensation of 2,6-diformyl-*p*-cresol and 3,6-dioxaoctane-1,8-diamine in the presence of appropriate quantities of the heterolanthanide nitrates as described previously.<sup>12</sup> The complexes were examined on the microscope for homogeneity in crystal morphology and similarity to the well characterized homodinuclear complexes  $\text{Ln}_2\text{L}(\text{NO}_3)_4 \cdot \text{H}_2\text{O}$ <sup>12</sup> (Fig. 1).

**Neutron Activation Analysis (NAA).**—The concentrations of

† Non-SI unit employed:  $\text{eV} \approx 1.6 \times 10^{-19} \text{ J}$ .

**Table 1** Mole fraction of europium ( $x_{Eu}$ ) [or terbium ( $x_{Tb}$ )] and the heterolanthanide ( $x_{Ln}$ ) found by neutron activation analysis for crystalline  $(Ln_{1-x}Eu_x)_2L(NO_3)_4 \cdot H_2O$  or  $(Ln_{1-x}Tb_x)_2L(NO_3)_4 \cdot H_2O$  complexes obtained from solutions containing  $0.5x_{Eu}$  (or  $0.5x_{Tb}$ ) and  $0.5x_{Ln}$ . The lanthanide(III) cation radii,  $r_{Ln}$ , in six-co-ordination<sup>23</sup> are also given

Ln	$(Ln_{1-x}Eu_x)_2L(NO_3)_4 \cdot H_2O$		$(Ln_{1-x}Tb_x)_2L(NO_3)_4 \cdot H_2O$		$r_{Ln}/\text{\AA}$
	$x_{Eu}$	$x_{Ln}$	$x_{Tb}$	$x_{Ln}$	
La	0.49	0.51			1.061
Ce	0.47	0.50	0.20	0.91	1.034
Pr	0.62	0.38	0.22	0.74	1.031
Nd	0.51	0.41	0.21	0.84	0.995
Sm	0.38	*	0.24	*	0.964
Eu			0.26	0.74	0.950
Gd	0.45	*	0.29	*	0.938
Tb	0.74	0.26			0.923
Dy	0.76	*	0.57	*	0.908

\* Element was not quantified.

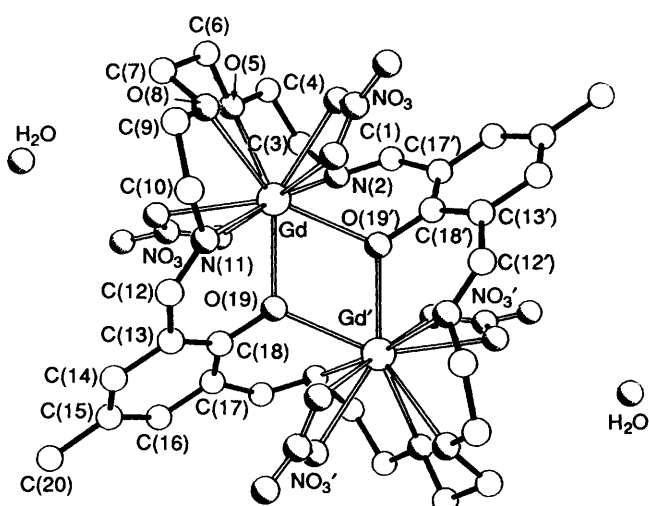


**Fig. 1** The molecular structure of dinuclear  $Ln_2L(NO_3)_4 \cdot H_2O$  complexes. A representative gadolinium structure is shown<sup>5,21</sup>

lanthanum, praseodymium, neodymium, europium and terbium were determined by neutron activation analyses at the University of the West Indies (UWI) Center for Nuclear Sciences. Irradiations were carried out in a small pool-type light-water cooled and moderated SLOWPOKE-II research reactor, having a maximum rated flux of  $10^{12}$  neutrons  $cm^{-2} s^{-1}$ . The spectra were measured and analysed on a gamma spectrometry system consisting of an Ortec high purity germanium coaxial detector (relative efficiency 15% and resolution 1.8 keV at 1.33 MeV), multichannel buffer and GELIGAM software package. The standards used were supplied by Aldrich and the results (Table 1) were in good agreement with those obtained by Inductively Coupled Plasma (ICP) methods (Galbraith Laboratories Inc., Knoxville, TN).

**Luminescence Lifetime Measurements.**—The luminescence lifetimes were determined using either the set-up at Tulane University which was described previously<sup>22</sup> or the new system at the UWI. The UWI facility utilises a pulsed Photon Technology International (PTI) PL 2300 nitrogen laser (pulse width <1 ns, and maximum energy 1.4 mJ per pulse) which pumps a PL201 dye laser. The observation wavelength for sample emission was selected on a quarter meter PTI S/N 1137 monochromator ( $600 g mm^{-1}$ , blazed at 500 nm and aperture ratio  $f = 2.5$ ). The emission was detected by a Hamamatsu R928 photomultiplier tube and then passed through an NE 531N preamplifier from R.S. Components Ltd. which was sampled by a Tektronics 2232 oscilloscope (100 mHz bandwidth, 100 megasamples  $s^{-1}$ , 1000 channels, 8 bit digitizer and

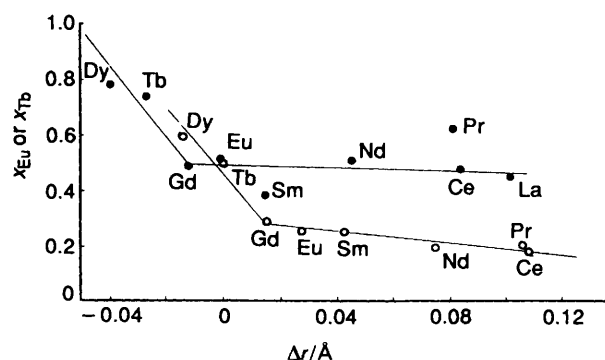


**Fig. 2** The dependence of  $Eu^{3+}$  and  $Tb^{3+}$  mole fractions in the crystalline heterolanthanide products on the ionic radii difference,  $\Delta r$  [ $\Delta r = r(Ln^{3+}) - r(Eu^{3+}$  or  $Tb^{3+})$ ],  $(Ln_{1-x}Eu_x)_2L(NO_3)_4 \cdot H_2O$  (●) and  $(Ln_{1-x}Tb_x)_2L(NO_3)_4 \cdot H_2O$  (○)

16 bit storage amplitude resolution). The scope was triggered by a PTI photodiode detector placed in the excitation beam. Generally, about 1000 transients were averaged by the scope, transferred to a 386 PC computer for further averaging and/or analysis using a non-linear Marquardt procedure.<sup>23</sup> Parameters obtained using the two set-ups were essentially similar.

For 77 K measurements, the samples were sealed in 4 mm glass tubes and placed in a 50  $cm^3$  finger type quartz EPR dewar. Selective excitation of  $Eu^{3+}$  ( $^5D_0$ ) at 575.9 nm was accomplished with Rhodamine 6G (one stock solution was used throughout to optimize reproducibility of background effects);  $Tb^{3+}$  was indiscriminately excited at 337 nm since excitation at 488 nm gave very low emission intensity.

## Results and Discussion

**Distribution of  $Eu^{3+}$  in the  $(Ln_{1-x}Eu_x)_2L(NO_3)_4 \cdot H_2O$  Heterodinuclear Complexes.**—Reaction mixtures containing equimolar amounts of  $Eu^{3+}$  and  $Ln^{3+}$  ( $Ln = La-Dy$ , except Pm) deposited crystalline  $(Ln_{1-x}Eu_x)_2L(NO_3)_4 \cdot H_2O$  complexes which exhibited variable compositions depending on the nature of  $Ln^{3+}$  (Table 1). The measured mole fractions of  $Eu^{3+}$  ( $x_{Eu}$ ) relative to the total lanthanide concentration in the crystalline products, i.e.  $x$  in the formula  $(Ln_{1-x}Eu_x)_2L(NO_3)_4 \cdot H_2O$ , are plotted against the cation radii difference  $\Delta r$  ( $\Delta r =$  radius of  $Ln^{3+} -$  radius of  $Eu^{3+}$ ) in Fig. 2. All radii used are empirical averages of  $Ln^{3+}$  in six-co-ordination derived from many structures<sup>24</sup> and often used for comparative purposes.<sup>25</sup> The measured europium levels are generally in the range  $x \approx 0.4-0.6$  when the competing heterocations,  $Ln^{3+}$ , are members of the large lanthanide series ( $Ln = La-Gd$ ). But with members of the small lanthanide series,  $Ln = Tb^{3+}$  and  $Dy^{3+}$ , preferential

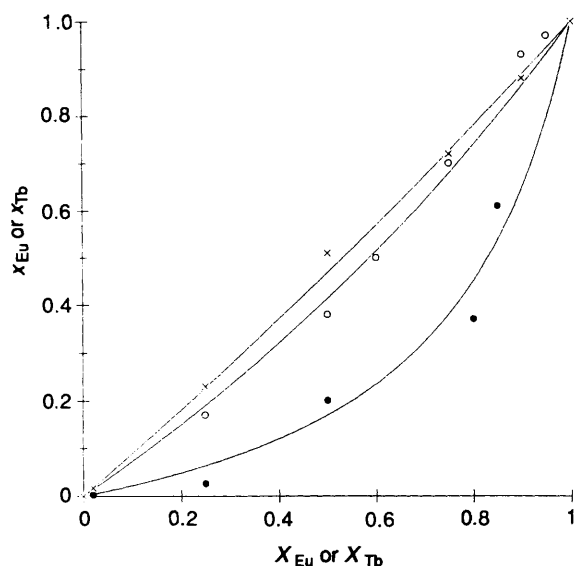


Fig. 3 The dependence of the mole fraction ( $x_{Eu}$ ) of  $Eu^{3+}$  (or  $x_{Tb}$  of  $Tb^{3+}$ ) in the crystalline  $(Ln_{1-x}Eu_x)_2L(NO_3)_4 \cdot H_2O$  and  $(Ln_{1-x}Tb_x)_2L(NO_3)_4 \cdot H_2O$  on the initial mole fraction ( $X_{Eu}$  of  $Eu^{3+}$  (or  $X_{Tb}$  of  $Tb^{3+}$ ) in the parent reaction mixture. Lines show best fits to equation (1); Nd-Tb (●), Sm-Eu (○), Nd-Eu (×)

enrichment of  $Eu^{3+}$  is observed. Molecular recognition processes which govern the template condensation of 2,6-diformyl-*p*-cresol with 3,6-dioxaoctane-1,8-diamine to yield L and its dilanthanide complexes are on the basis of these results more selective towards the larger  $Ln^{3+}$  cations. The deviant behaviour of samarium and praseodymium compounds does not have an obvious explanation but reflects a selectivity differential. The preference for large  $Ln^{3+}$  cations by either L or key intermediates along the cyclic Schiff-base formation reaction pathway was studied in detail using reaction mixtures with widely varying europium concentrations.

The mole fraction of  $Eu^{3+}$ ,  $x_{Eu}$ , in the solid products  $(Ln_{1-x}Eu_x)_2L(NO_3)_4 \cdot H_2O$ ,  $Ln = Nd$  or  $Sm$ , is plotted against the initial mole fraction of  $Eu^{3+}$  in the mother-reaction mixture,  $X_{Eu}$ , in Fig. 3. The good linear relationship between  $x_{Eu}$  and  $X_{Eu}$  for  $(Nd_{1-x}Eu_x)_2L(NO_3)_4 \cdot H_2O$  complexes over the entire range of  $X_{Eu}$  (0–1.0) confirms that  $Nd^{3+}$  and  $Eu^{3+}$  form complexes of similar stabilities during events in which  $Ln^{3+}$  ion-pairing mechanisms are active. However, unexpectedly, the relationship between  $x_{Eu}$  and  $X_{Eu}$  for the  $(Sm_{1-x}Eu_x)_2L(NO_3)_4 \cdot H_2O$  complexes (Fig. 3) is not linear, although  $Eu^{3+}$  and  $Sm^{3+}$  ( $\Delta r = 0.015 \text{ \AA}$ ) being more similar in size than  $Eu^{3+}$  and  $Nd^{3+}$  ( $\Delta r = 0.045 \text{ \AA}$ ) would be expected to fit better in the identical co-ordination cavities of L. Instead, the solid products,  $(Sm_{1-x}Eu_x)_2L(NO_3)_4 \cdot H_2O$  (Fig. 3) have larger Sm:Eu concentration ratios compared to that of the mother-reaction mixture. This behaviour is inconsistent with what would be expected on the basis of usual lanthanide contraction effects.<sup>25</sup> Since both  $Sm_2$  and  $Eu_2$  homopairs are complexed by L efficiently,<sup>12</sup> the contrasting behaviour of the Nd-Eu and Sm-Eu systems reflects the importance of co-operative heteropair properties to competitive complexation. For a better understanding of this behaviour we studied the  $(Ln_{1-x}Tb_x)_2L(NO_3)_4 \cdot H_2O$  complexes in which the  $Tb^{3+}$  cation is smaller than  $Eu^{3+}$ .

**Distribution of  $Tb^{3+}$  in Heterodilanthanide  $(Ln_{1-x}Tb_x)_2L(NO_3)_4 \cdot H_2O$  Complexes.**—The mole fraction of  $Tb^{3+}$ ,  $x_{Tb}$ , in the crystalline  $(Ln_{1-x}Tb_x)_2L(NO_3)_4 \cdot H_2O$  complexes which were obtained from parent-reaction mixtures containing equimolar amounts of  $Ln^{3+}$  and  $Tb^{3+}$  are plotted against the radii difference  $\Delta r$  in Fig. 2. Preferential incorporation of the large lanthanide cations into the solid  $(Ln_{1-x}Tb_x)_2L(NO_3)_4 \cdot H_2O$

complexes is evident from the small values of  $x_{Tb}$  ( $0.20 < x_{Tb} < 0.30$ , Table 1). There is a slight systematic increase in the concentration of  $Tb^{3+}$  on going from  $Ce^{3+}$  to  $Gd^{3+}$ , but with small  $Ln^{3+}$  ions,  $Ln = Gd$ – $Dy$ , the heterodilanthanide crystalline products become increasingly richer in  $Tb^{3+}$ .

The  $(Nd_{1-x}Tb_x)_2L(NO_3)_4 \cdot H_2O$  system, featuring  $Ln^{3+}$  cations of vastly contrasting radii, was studied in detail. The mole fractions of  $Tb^{3+}$  in the solid products,  $x_{Tb}$ , are plotted against the mole fraction of  $Tb^{3+}$ ,  $X_{Tb}$ , in the parent-reaction mixtures in Fig. 3. The solid products are richer in  $Nd^{3+}$  for  $X_{Tb} < 0.8$ , but preferential incorporation of  $Tb^{3+}$  is evident for  $X_{Tb} > 0.8$ . Indeed, the behaviour of the  $(Nd_{1-x}Tb_x)_2L(NO_3)_4 \cdot H_2O$  compounds is similar to that of  $(Sm_{1-x}Eu_x)_2L(NO_3)_4 \cdot H_2O$  complexes with preference for the large  $Nd^{3+}$  ion more dramatically expressed. The competitive behaviour of the homo- and hetero-pairs towards L is compared below.

**Partition of Lanthanide(III) Cations Between Solubilized Species and Crystalline Heterodilanthanide Complexes.**—The distribution of lanthanide cations  $Ln^{3+}$  between the numerous uncharacterized solubilized species retained by the reaction mother-liquor and the well defined crystalline products  $(Ln^A_{1-x}Ln^B_x)_2L(NO_3)_4 \cdot H_2O$  may be described in detail by the partition law. Phenomenologically, the observed mole fraction of  $Ln^A$  in the crystalline product is adequately described by equation (1) where  $x_A$  is the mole fraction of  $Ln^A$  in the

$$x_A = (X_A p_A) / (X_A p_A + X_B p_B) \quad (1)$$

crystalline product,  $X_A$  and  $X_B$  are the initial mole fractions of  $Ln^A$  and  $Ln^B$  in the mother-reaction mixture and  $p_A$  and  $p_B$  are probabilities for the incorporation of  $Ln^A$  and  $Ln^B$  respectively into the crystalline products. For comparative purposes we define a cation discrimination index  $I_D = p_A/p_B$ , where  $Ln^A$  is the larger of the two lanthanide cations competing for complexation.

With  $(Sm_{1-x}Eu_x)_2L(NO_3)_4 \cdot H_2O$  (Fig. 3) use of a non-linear Marquardt least-squares curve fitting procedure yields the constants  $p_{Sm}$  and  $p_{Eu}$  from which the cation discrimination index  $I_D = p_{Sm}/p_{Eu} = 1.5$  is derived. Indeed samarium(III) is a better competitor (Fig. 2) for complexation than the other larger lanthanide(III) cations. For complexes in which the radii of the competing cations are vastly different, as in  $(Nd_{1-x}Tb_x)_2L(NO_3)_4 \cdot H_2O$  (Fig. 3) the corresponding lanthanide(III) cation discrimination index,  $I_D = p_{Nd}/p_{Tb} = 5$ , is dramatically much larger.

The above macroscopic characteristics show conclusively that co-ordination of competing hetero  $Ln^{3+}$  cations by dinucleating chelate L defies a simple dependence on  $Ln^{3+}$  cation size and demonstrate the overriding importance of co-operative heteropair effects. Formation of heteropaired molecules, such as  $SmEuL(NO_3)_4 \cdot H_2O$ , is thus implied though not proved. An investigation of the microscopic environments of the individual hetero ions is required to prove the formation of heteropaired molecules. This was done for  $(Sm_{1-x}Eu_x)_2L(NO_3)_4 \cdot H_2O$  using  $Eu^{3+}$  ions as luminescent probes.<sup>2-6</sup>

**Luminescence Decay Dynamics of  $Eu^{3+}$  ( $^5D_0$ ) in  $(Sm_{1-x}Eu_x)_2L(NO_3)_4 \cdot H_2O$  at 77 K.**—The luminescence spectra of  $(Sm_{1-x}Eu_x)_2L(NO_3)_4 \cdot H_2O$  are dominated by strong emission from the  $^5D_0$  level of  $Eu^{3+}$  at 77 K (Fig. 4). The emission from the  $^4G_3$  state of  $Sm^{3+}$  which was observed<sup>21</sup> at both 298 and 77 K is apparently quenched by  $Eu^{3+}$ . The emission decay rate constants and integrated intensities of  $Eu^{3+}$  emission are given in Table 2. The luminescence decay rate constant of  $Eu^{3+}$  in the absence of  $Sm^{3+}$  ( $k_0$ ) is  $\approx 1140 \text{ s}^{-1}$  and is independent of temperature (for  $T < 110 \text{ K}$ ) and concentration quenching effects.<sup>21</sup> For the  $(Sm_{1-x}Eu_x)_2L(NO_3)_4 \cdot H_2O$  complexes, the largely non-exponential behaviour of the luminescence decay of  $Eu^{3+}$  in the region  $0 < x_{Eu} < 0.75$  is evident in Table 2 and Fig. 5. The short-lived luminescence has a decay rate constant

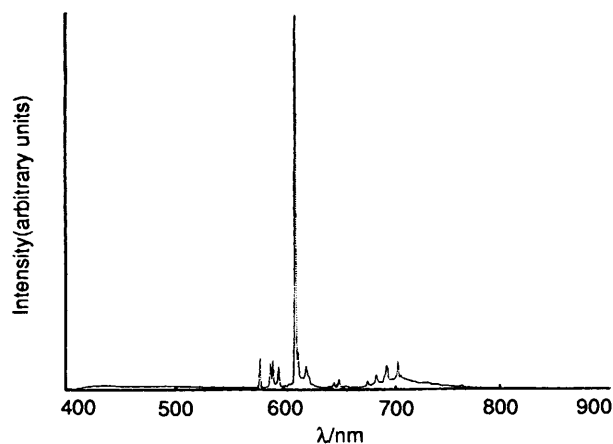


Fig. 4 The luminescence spectrum of the  $(\text{Sm}_{0.6}\text{Eu}_{0.4})_2\text{L}(\text{NO}_3)_4\cdot\text{H}_2\text{O}$  complex at 77 K, following excitation at 350 nm

**Table 2** Initial mole fraction of europium ( $X_{\text{Eu}}$ ) [or terbium ( $X_{\text{Tb}}$ )] in the reaction mixture and the corresponding mole fraction of europium ( $x_{\text{Eu}}$ ) [or terbium ( $x_{\text{Tb}}$ )] in the isolated compounds; luminescence decay constants ( $k_1$  and  $k_2$ ) and integrated intensities ( $I_0$ ) at 77 K (see text)

$(\text{Sm}_{1-x}\text{Eu}_x)_2\text{L}(\text{NO}_3)_4\cdot\text{H}_2\text{O}$

$X_{\text{Eu}}$	$x_{\text{Eu}}$	$k_1/\text{s}^{-1}$	$k_2/\text{s}^{-1}$	$10^4 I_0^a$
1.00	1.00		1140	8.17
0.95	0.97		1210	7.69
0.90	0.93		1260	6.81
0.85	0.87 <sup>b</sup>		1320	7.21
0.75	0.70		1420	5.69
0.60	0.50	7900	1410	4.72
0.50	0.38	7600	1460	4.04
0.43	0.30 <sup>b</sup>	6900	1320	3.24
0.30	0.20 <sup>b</sup>	8300	1420	3.60
0.25	0.17	8300	1400	2.58
0.15	0.10 <sup>b</sup>	8600		1.72
0.05	0.03 <sup>b</sup>			1.45

$(\text{Nd}_{1-x}\text{Eu}_x)_2\text{L}(\text{NO}_3)_4\cdot\text{H}_2\text{O}$

$X_{\text{Eu}}$	$x_{\text{Eu}}$	$x_{\text{Nd}}$	$X_{\text{Tb}}$	$x_{\text{Tb}}$	$x_{\text{Nd}}$
0.02	0.017	1.00	0.02	0.002	0.78
0.25	0.23	0.82	0.25	0.026	1.07
0.50	0.51	0.41	0.50	0.20	0.81
0.75	0.72	0.27	0.80	0.37	0.63
0.90	0.79	0.12	0.85	0.61	0.37

<sup>a</sup> Emission monitored at 612 nm following excitation at 575.9 nm.

<sup>b</sup> Concentrations calculated using equation (1) (Fig. 1).

$k_1 \approx 8200 \text{ s}^{-1}$  while the cumulative average decay rate constant for the long-lived components is  $k_2 \approx 1400 \text{ s}^{-1}$ . These results do confirm that europium ions are in two different environments. We attribute the fast decaying emission ( $k_1$ ) to intramolecularly coupled  $\text{Eu}^{3+}$ – $\text{Sm}^{3+}$  heteropairs in  $\text{SmEuL}(\text{NO}_3)_4\cdot\text{H}_2\text{O}$  heterolanthanide molecules. The cumulative long-lived average ( $k_2$ ) is due to  $\text{Eu}^{3+}$ – $\text{Eu}^{3+}$  homopairs intermolecularly coupled to  $\text{Sm}^{3+}$ – $\text{Sm}^{3+}$  or  $\text{Sm}^{3+}$ – $\text{Eu}^{3+}$  pairs in neighbouring  $\text{Sm}_2\text{L}(\text{NO}_3)_4\cdot\text{H}_2\text{O}$  homodinuclear or  $\text{SmEuL}(\text{NO}_3)_4\cdot\text{H}_2\text{O}$  heterodinuclear molecules. Energy transfer efficiency  $\eta$  as given by the expression  $1 - (k_0/k) \approx 0.86$  for intramolecularly coupled  $\text{Sm}^{3+}$ – $\text{Eu}^{3+}$  heteropairs ( $k = k_1$ ) in which the cations are linked by a phenolate oxygen bridge at  $\approx 4.0 \text{ \AA}$  and for intermolecularly coupled ( $k = k_2$ )  $\text{Sm}$ – $\text{Eu}$  pairs  $\eta = 0.19$ .

The negligible variations in  $k_2$  for all  $X_{\text{Eu}} < 0.75$  (Table 1) suggests that intermolecular interactions are limited to a few neighbours. The relatively low  $\text{Eu}^{3+}$  to  $\text{Sm}^{3+}$  energy transfer efficiency for both intra- and inter-molecular processes makes energy transfer by exchange mechanisms unlikely. Energy trans-

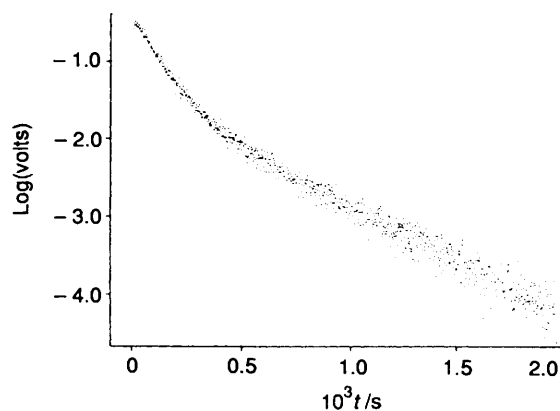


Fig. 5 The biphasic behaviour of the luminescence decay dynamics of  $\text{Eu}^{3+}$  ( $^4\text{D}_0$ ) in  $(\text{Sm}_{0.3}\text{Eu}_{0.7})_2\text{L}(\text{NO}_3)_4\cdot\text{H}_2\text{O}$ ; fast decay,  $k_1 \approx 8200 \text{ s}^{-1}$  and slow decay,  $k_2 \approx 1400 \text{ s}^{-1}$

fer through multipolar interactions appears more likely. Diffusion limited processes are unimportant since  $\text{Eu}^{3+}$  to  $\text{Nd}^{3+}$  energy transfer in isostructural  $(\text{Nd}_{1-x}\text{Eu}_x)_2\text{L}(\text{NO}_3)_4\cdot\text{H}_2\text{O}$  is much faster (see below). Assuming energy transfer by predominantly dipole–dipole mechanisms in the fast diffusion limit,<sup>5</sup> the energy transfer rate constant  $k_{\text{DD}}$  is given by equation (2) which

$$k_{\text{DD}} = 6.023 \times 10^{-1} \int_0^\infty k_0(r/R_0)^{-6} (4\pi r^2) dr \quad (2)$$

simplifies to equation (3) where,  $R_0 = 50\%$  transfer distance

$$k_{\text{DD}} = 2883 R_0^6/a^3 \quad (3)$$

(nm) for a single donor–acceptor pair and  $a =$  donor–acceptor distance of closest approach. The value of  $a$  is well defined for the heteropair,  $\text{Sm}^{3+}$ – $\text{Eu}^{3+}$ , *i.e.*  $\approx 4 \text{ \AA}$ , therefore  $R_0 \approx 0.73 \text{ nm}$  ( $k_{\text{DD}(1)} \approx 7054 \text{ s}^{-1}$  from the relation  $k_{\text{DD}(1)} = k_1 - k_0$ ).

The crystal structure of  $\text{Ln}_2\text{L}(\text{NO}_3)_4\cdot\text{H}_2\text{O}$ <sup>12,21</sup> exhibits the following intermolecular  $\text{Ln} \cdots \text{Ln}$  contacts  $< 1.8 \text{ nm}$  (nm with the number of contacts in parentheses): 0.85(1), 0.92(2), 1.04(4), 1.12(4), 1.16(2), 1.18(2), 1.22(2), 1.24(3), 1.35(1), 1.44(2), 1.56(1), 1.58(4), 1.65(6), 1.74(2), 1.78(4), 1.80(3). The measured constant value of  $k_2 \approx 1400 \text{ s}^{-1}$  leads to  $k_{\text{DD}(2)} = 263 \text{ s}^{-1}$  for the slowly decaying component which corresponds to a distance of closest intermolecular approach of  $a = 1.18 \text{ nm}$ . This distance is not compatible with the presence of the much shorter  $\text{Sm} \cdots \text{Eu}$  intermolecular contacts. Therefore the measured constant intermolecular energy transfer rate of  $k_{\text{DD}(2)} (= k_2 - k_0) \approx 263 \text{ s}^{-1}$  must be a weighted average of several processes within a limited volume. A weighted average of  $k_{\text{DD}} = 247 \text{ s}^{-1}$  is obtained using equation (3), with  $R_0 = 0.73 \text{ nm}$  and all intermolecular contacts, for which  $a \leq 1.74 \text{ nm}$ . On the basis of these results, it is concluded that the crystalline  $(\text{Sm}_{1-x}\text{Eu}_x)_2\text{L}(\text{NO}_3)_4\cdot\text{H}_2\text{O}$  complexes contain heterolanthanide molecules  $\text{SmEuL}(\text{NO}_3)_4\cdot\text{H}_2\text{O}$  in which the intramolecular  $\text{Sm}^{3+}$ – $\text{Eu}^{3+}$  interaction is relatively weak. There are also  $\text{Eu}_2\text{L}(\text{NO}_3)_4\cdot\text{H}_2\text{O}$  and  $\text{Sm}_2\text{L}(\text{NO}_3)_4\cdot\text{H}_2\text{O}$  homodinuclear molecules present and exhibiting very weak mutual intermolecular coupling. Assuming predominantly dipolar interactions, the intramolecular  $\text{Sm}$ – $\text{Eu}$  coupling constant ( $\alpha$ ) is, from  $k_{\text{DD}} = \alpha/R^6$ ,  $2.9 \times 10^{-53} \text{ m}^6 \text{ s}^{-1}$ .

Support for these conclusions is found in a comparison of luminescence integrated intensities. When intermolecular interactions are ignored, integrated intensities ( $I$ ) can be described by equation (4)<sup>27</sup> where  $I_0$  is the integrated luminescence

$$I = I_0 X_{\text{EuEu}}^2 + I_h X_{\text{EuSm}}^2 + c_0 \quad (4)$$

intensity in the absence of  $\text{Sm}^{3+}$  (*i.e.* of unperturbed  $\text{Eu}$ – $\text{Eu}$  homopairs),  $I_h$  is the integrated luminescence intensity due to coupled  $\text{Eu}$ – $\text{Sm}$  ions in  $\text{SmEuL}(\text{NO}_3)_4\cdot\text{H}_2\text{O}$  molecules

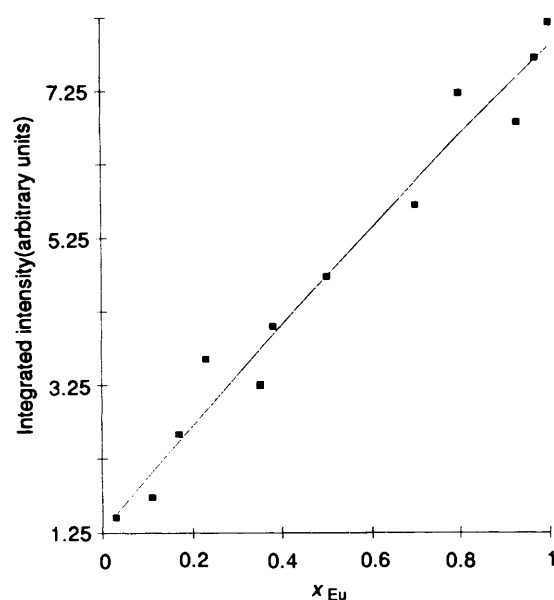


Fig. 6 The dependence of the luminescence integrated intensity,  $I_0 = \sum_{i=0}^{\infty} I_i$  of  $\text{Eu}^{3+}$ , at 77 K following excitation of the  $^5\text{D}_0$  state at 575.9 nm, on the mole fraction of  $\text{Eu}^{3+}$  in crystalline  $(\text{Sm}_{1-x}\text{Eu}_x)_2\text{L}(\text{NO}_3)_4 \cdot \text{H}_2\text{O}$  complexes. The line shows best fit to equation (5)

(approximated as  $I_h \approx I_0 k_1/k_0$ ),  $X_{\text{EuEu}}$  is the mole fraction of Eu–Eu homopairs,  $X_{\text{EuSm}}$  is the mole fraction of Eu–Sm heteropairs and  $c_0$  is the cumulative intensity due to background effects.

The mole fraction of Eu–Eu homopairs is dependent on the mole fraction of europium, therefore  $X_{\text{EuEu}} = (c_1/2)x_{\text{Eu}}$  and the mole fraction of the Eu–Sm heteropairs depends on the population of both Sm and Eu, hence  $X_{\text{EuSm}} = c_2(x_{\text{Sm}}x_{\text{Eu}})^{1/2}$ ,  $c_1$  and  $c_2$  are ion pairing selectivity constants for the homo- and hetero-pair respectively. Equation (4) can be rewritten in terms of equation (5).

$$I = I_0(c_1/2)^2 x_{\text{Eu}}^2 + I_h c_2^2 x_{\text{Eu}}(1 - x_{\text{Eu}}) + c_0 \quad (5)$$

Observed integrated luminescence intensities are plotted against the mole fraction of  $\text{Eu}^{3+}$  ( $x_{\text{Eu}}$ ) in Fig. 6. From equation (5), the ratio of  $c_1$  to  $c_2$  is approximately 1:1.5 which is larger than the value of 1:2.0 expected for a process in which EuEu, EuSm and SmSm pairing is purely statistical. These results support the conclusion that the formation of dinuclear lanthanide complexes of chelate L is governed by molecular recognition processes in which the homo- or hetero-lanthanide cations are recognized and paired on the basis of their co-operative effects the detailed nature of which is of great interest.

The 77 K decay curves in the case of  $(\text{Nd}_{1-x}\text{Eu}_x)_2\text{L}(\text{NO}_3)_4 \cdot \text{H}_2\text{O}$  are non-exponential and energy transfer is very fast and efficient (study in progress). Presumably, this is because of the presence of a hypersensitive energy level ( $^2\text{G}_7$ ) on  $\text{Nd}^{3+}$  which matches well the energy of the  $^5\text{D}_0$  state of  $\text{Eu}^{3+}$  and is therefore better placed for efficient resonant energy transfer.

The behaviour of the  $(\text{Tb}_{1-x}\text{Pr}_x)_2\text{L}(\text{NO}_3)_4 \cdot \text{H}_2\text{O}$  system is somewhat similar to that of the  $(\text{Sm}_{1-x}\text{Eu}_x)_2\text{L}(\text{NO}_3)_4 \cdot \text{H}_2\text{O}$  complexes. Detailed studies were limited by poor emission when the  $^5\text{D}_4$  state of  $\text{Tb}^{3+}$  was directly excited. However, indiscriminate excitation at 337 nm yields  $12\,500\text{ s}^{-1}$  for the decay rate constant of the short-lived component attributable to  $\text{Pr}^{3+}$ – $\text{Tb}^{3+}$  heteropairs. The  $\text{Tb}^{3+}$ – $\text{Pr}^{3+}$  intramolecular interaction ( $\alpha = 4.7 \times 10^{-53}\text{ m}^6\text{ s}^{-1}$ ) is as moderate as that of  $\text{Sm}^{3+}$ – $\text{Eu}^{3+}$  heteropairs.

In conclusion, studies of the microscopic electronic environ-

ments of  $\text{Eu}^{3+}$  and  $\text{Tb}^{3+}$  ions confirm the formation of hetero-lanthanide(III) cation pairs which are weakly coupled by mainly dipolar interactions.

### Acknowledgements

We thank the University of the West Indies Postgraduate and Research Publications Committees, Louisiana Board of Regents (LEQSF grants), the British Council, the Third World Academy of Sciences and the Royal Society of Chemistry for financial support, Professor Gerald Lalor (UWI, Center for Nuclear Sciences) for helpful discussion and Professor Colin D. Flint for designing the operational amplifier built by P. O'Grady.

### References

- 1 R. D. Lauffer, *Chem. Rev.*, 1987, **87**, 901.
- 2 P. S. Richardson, *Chem. Rev.*, 1982, **82**, 541.
- 3 W. deW. Horrocks, jun. and M. Albin, *Prog. Inorg. Chem.*, 1984, **1**.
- 4 V. Balzani and F. Scandola, *Supramolecular Photochemistry*, Ellis Horwood, Chichester, 1991.
- 5 C. F. Meares, S. M. Yeh and L. Stryer, *J. Am. Chem. Soc.*, 1981, **103**, 1607.
- 6 J.-M. Lehn, *Angew. Chem., Int. Ed. Engl.*, 1990, **29**, 1303.
- 7 L. M. Vallarino and R. C. Leif, PCT Int. Appl., WO89 11868 CLA61 K43100, 1989.
- 8 M. A. Burton, B. N. Gray, C. Jones and A. Coletti, *Nucl. Med. Biol.*, 1989, **16**, 495.
- 9 R. M. Izatt, R. Z. Brueling, M. L. Brueling, B. J. Tarbet, K. E. Krakowiak, J. S. Bradshaw and J. J. Christiansen, *Anal. Chem.*, 1988, **60**, 1825; *J. Chem. Soc., Chem. Commun.*, 1988, 812.
- 10 D. E. Fenton and P. A. Vigato, *Chem. Soc. Rev.*, 1988, **17**, 69.
- 11 I. A. Kahwa, J. Selbin, T. C.-Y. Hsieh and R. A. Laine, *Inorg. Chim. Acta.*, 1986, **118**, 179.
- 12 I. A. Kahwa, S. Folkes, D. J. Williams, S. V. Ley, C. A. O'Mahoney and G. L. McPherson, *J. Chem. Soc., Chem. Commun.*, 1989, 1531.
- 13 P. Guerriero, P. A. Vigato, J.-C. G. Bünzli and E. Moret, *J. Chem. Soc., Dalton Trans.*, 1990, 647.
- 14 P. Guerriero, S. Tamburini, P. A. Vigato and C. Bennelli, *Inorg. Chim. Acta*, 1991, **189**, 19.
- 15 J. M. Harrowfield, M. I. Ogden and A. H. White, *Aust. J. Chem.*, 1991, **44**, 1249.
- 16 I. A. Kahwa, J. Selbin, T. C.-Y. Hsieh and R. A. Laine, *Inorg. Chim. Acta*, 1988, **141**, 131; I. A. Kahwa, J. Selbin, T. C.-Y. Hsieh, D. W. Evans, K. M. Pamidimukkala and R. A. Laine, *Inorg. Chim. Acta*, 1988, **144**, 275.
- 17 P. Guerriero, S. Sitran, P. A. Vigato, C. Marega, A. Marigo and R. Zannetti, *Inorg. Chim. Acta*, 1990, **171**, 103; U. Cassellato, P. Guerriero, S. Tamburini, S. Sitran and P. A. Vigato, *J. Chem. Soc., Dalton Trans.*, 1991, 2141.
- 18 Z. J. Chao, C. Parent, G. LeFlem and P. Hagenmuller, *J. Solid State Chem.*, 1991, **93**, 17.
- 19 V. Balzani and R. Ballardini, *Photochem. Photobiol.*, 1990, **52**, 409.
- 20 G. Blasse, *Photochem. Photobiol.*, 1990, **52**, 417.
- 21 K. D. Matthews, S. A. Bailey-Folkes, I. A. Kahwa, G. L. McPherson, C. A. O'Mahoney, S. V. Ley, D. J. Williams, C. J. Groombridge and C. J. O'Connor, *J. Phys. Chem.*, 1992, **96**, 7021.
- 22 I. A. Kahwa, J. Selbin, C. J. O'Connor, J. W. Foise and G. L. McPherson, *Inorg. Chim. Acta*, 1988, **148**, 265.
- 23 D. W. Marquardt, *J. Soc. Ind. Appl. Math.*, 1963, **11**, 431.
- 24 R. D. Shannon and C. T. Prewitt, *Acta Crystallogr., Sect. B*, 1971, **25**, 925.
- 25 I. A. Kahwa, *J. Therm. Anal.*, 1982, **25**, 525; S. P. Sinha, *Structure Bonding (Berlin)*, 1975, **25**, 69; I. A. Kahwa, F. R. Fronczek and J. Selbin, *Inorg. Chim. Acta*, 1984, **82**, 167; F. A. Hart, in *Comprehensive Coordination Chemistry*, ed. G. Wilkinson, Pergamon, Oxford, 1987, vol. 3, p. 1059.
- 26 A. K. Banerjee, F. Stewart-Darling, C. D. Flint and R. W. Schwartz, *J. Phys. Chem.*, 1981, **85**, 146.
- 27 R. A. Auerbach and G. L. McPherson, *Phys. Rev. B*, 1986, **33**, 6815.

Received 9th October 1992; Paper 2/05412D